

# Magnetic versus non-magnetic pinning of vortices in superconducting films: Role of effective penetration depth

J. del Valle', A. Gomez', E. M. Gonzalez, and J. L. Vicent'

Citation: *Appl. Phys. Lett.* **109**, 172601 (2016); doi: 10.1063/1.4966222

View online: <http://dx.doi.org/10.1063/1.4966222>

View Table of Contents: <http://aip.scitation.org/toc/apl/109/17>

Published by the [American Institute of Physics](#)

---

---

## Magnetic versus non-magnetic pinning of vortices in superconducting films: Role of effective penetration depth

J. del Valle,<sup>1,a)</sup> A. Gomez,<sup>1,b)</sup> E. M. Gonzalez,<sup>1,2</sup> and J. L. Vicent<sup>1,2,c)</sup>

<sup>1</sup>Departamento Física Materiales, Facultad CC. Físicas, Universidad Complutense, Madrid 28040, Spain

<sup>2</sup>IMDEA-Nanociencia, c/Faraday 8, Cantoblanco 28049, Madrid, Spain

(Received 23 July 2016; accepted 14 October 2016; published online 24 October 2016)

In order to compare magnetic and non-magnetic pinning, we have nanostructured two superconducting films with the regular arrays of pinning centers: Cu (non-magnetic) dots in one case and Py (magnetic) dots in the other. For low applied magnetic fields, when all the vortices are pinned in the artificial inclusions, the magnetic dots prove to be better pinning centers, as has been generally accepted. Unexpectedly, when the magnetic field is increased and interstitial vortices appear, the results are very different: we show how the stray field generated by the magnetic dots can produce an effective reduction of the penetration length. This results in strong consequences in the transport properties, which, depending on the dot separation, can lead to an enhancement or worsening of the transport characteristics. Therefore, the election of the magnetic or non-magnetic character of the pinning sites for an effective reduction of dissipation will depend on the range of the applied magnetic field. *Published by AIP Publishing.* [<http://dx.doi.org/10.1063/1.4966222>]

Vortex dynamics in superconducting thin films have been subject of intense research during last years.<sup>1–3</sup> Lithography techniques have allowed to nanostructure these films with sizes similar to the superconducting characteristic lengths, deeply affecting vortex pinning potentials and, hence, transport properties of the superconductor. As a result, a variety of new phenomena have been observed, such as commensurability,<sup>1</sup> ratchet<sup>2</sup> or guided motion effects.<sup>4</sup> The effect of mesoscopic magnetic inclusions on the superconducting properties has been thoroughly studied.<sup>5</sup> Interplay between magnetism and superconductivity has led to the appearance of novel behaviors, such as field induced superconductivity,<sup>6</sup> which is based on nanoengineering the magnetic field experienced by the superconductor, where also vortex-antivortex phenomena play important role,<sup>7</sup> as well as their behavior in the presence of applied drive<sup>8</sup> and pinning of vortices on ferromagnetic domains and domain walls.<sup>9</sup> Finally, worth to notice that promising applications as memory or sensing devices<sup>10</sup> can be achieved with the appropriate hybrid systems. Despite all this progress, the fundamental problem of which is the best way to reduce dissipation in superconductors is still an open subject of great technological interest.

Recently, some authors have addressed the problem of the optimum geometry, finding that a graded pinning landscape provides the best transport properties over a broad range of magnetic fields.<sup>11,12</sup> Yet, it is still uncertain which kind of materials should be used to induce effective pinning landscapes. Most authors have found magnetic inclusions to provide stronger individual vortex pinning than non-magnetic ones.<sup>13–15</sup> However, these magnetic pinning centers do not necessarily mean less dissipation,<sup>16</sup> since at high

applied magnetic fields most vortices occupy interstitial positions and are not directly pinned by the artificial pinning centers, but by elastic strains of the vortex lattice. In this case, the onset of dissipation might be determined by the elastic softening of the vortex lattice. How the magnetism of the inclusions can affect this softening is a problem that had not been addressed yet, despite being the key to achieve better transport properties in a broad field range. In this paper, we compare the magnetotransport properties of two nanostructured Nb thin films: one with an array of non-magnetic Cu dots and the other with an identical array of magnetic Permalloy (Py) dots. While the Py dots sample shows better pinning properties at low fields, we show that stray fields can produce an effective decrease of the penetration length, profoundly affecting vortex dynamics at higher fields: this can enhance or worsen transport properties over an order of magnitude, depending on the dot spacing. These results prove the great impact of the magnetism on the interstitial vortex dynamics and reveal that the optimum pinning geometry is very dependent on the magnetic character of the inclusions.

Both samples are based on a rectangular ( $a = 400$  nm,  $b = 600$  nm) array of nanodots (200 nm diameter and 40 nm thickness) fabricated using electron beam lithography and magnetron sputtering (Cu in one case and Py in the another, see Fig. 1(a)). A 100 nm superconducting Nb thin film was grown on top of these arrays using magnetron sputtering in a chamber with base pressure  $5 \times 10^{-8}$  Torr ( $T_c = 8.5$  K, Fig. 1(a)). In order to test the interstitial vortex dynamics when pushed along the two different directions of the array, optical lithography and reactive ion etching were used to define a cross shaped, 40  $\mu$ m wide, bridge. Magnetotransport measurements have been carried out in a commercial Helium cryostat, with a 9T superconducting magnet and temperature stability better than  $\pm 2$  mK. The magnetic properties of the Py dots have been calculated using the OOMMF micromagnetic simulations. Fig. 1(b) shows the out of plane hysteresis loop of the Py dot as well as the  $M_z/M_s$  distribution inside the dot for

<sup>a)</sup>Present address: Department of Physics, University of California-San Diego, California 92093, USA.

<sup>b)</sup>Present address: Centro de Astrobiología, INTA-CSIC, 28850 Torrejón de Ardoz, Spain.

<sup>c)</sup>Author to whom correspondence should be addressed. Electronic mail: jlvicent@ucm.es

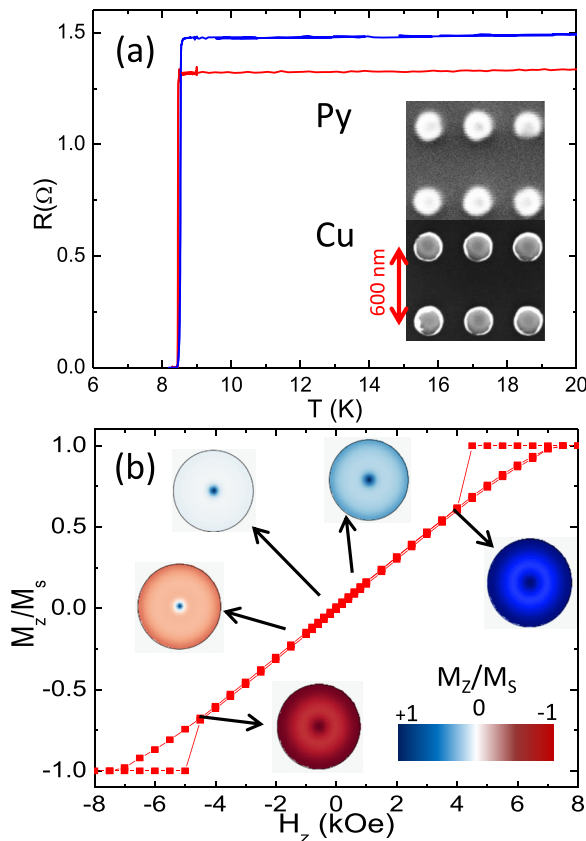


FIG. 1. (a) Superconducting transitions for the Cu (blue, upper curve) and Py (red, lower curve) nanodot samples. Inset: SEM image of the Cu and Py nanodot samples prior to Nb deposition. (b) Out of plane hysteresis loop of a Py nanodot obtained with the OOMMF simulations. The spatial distribution of  $M_z/M_s$  inside the dot is plotted for selected magnetic fields.

selected fields. Magnetization is arranged in a magnetic vortex configuration<sup>17</sup> with a small core, less than 10 nm. The reduced size of the core makes negligible its contribution to the total magnetization of the dot, and no asymmetries between positive or negative fields are observed when characterizing the magnetotransport properties. It can be observed that, for low fields, the out of plane magnetization takes place through progressive tilting of the magnetic moments surrounding the core, leading to a linear and reversible hysteresis loop around the measurement range of the superconducting properties ( $< 1$  kOe); i.e., no core inversion or expulsion of the core takes place during the measurements, and the symmetry of the pinning potential does not change,<sup>18</sup> but only the net magnetization.

Fig. 2 shows the critical currents of both samples as function of the temperature at the first matching field, when there is one vortex trapped in each dot ( $H_m = \phi_0 / (a \cdot b) = 87$  Oe). In this situation, the critical current is proportional to the pinning force, which is the same on each vortex. As observed in the previous studies,<sup>13–15</sup> magnetic dots work better as pinning centers, with critical currents considerably higher in the whole temperature range. As it is well known, vortices are surrounded by supercurrents that concentrate (screen) the magnetic field within (further than)  $\lambda$ , the penetration length of the superconductor. The stray field of a magnetized dot does precisely this effect: concentrating the flux inside the dot while screening it on the outside. For this reason, supercurrents will be weaker if a vortex is trapped on a magnetic dot

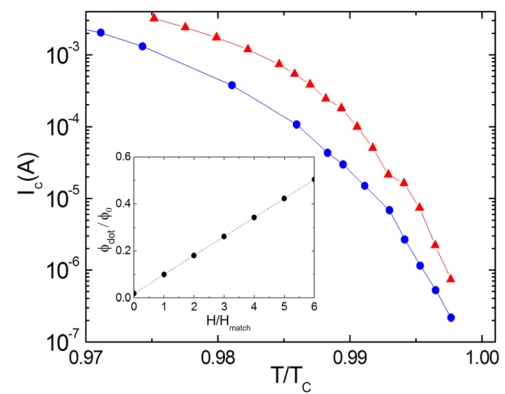


FIG. 2. Critical current (pushing vortices along the short side of the rectangular dot unit cell) as a function of the temperature for Cu (blue dots) and Py (red triangles) samples, after carefully trapping the magnetic field at  $H = H_m = 87$  Oe. Critical current criterion  $5 \mu\text{V}/\text{mm}$ . Inset: Stray field flux (normalized to  $\phi_0 = 2.07 \times 10^{-15}$  Wb) threading a Py dot as a function of the applied magnetic field (normalized to  $H_m$ ).

that if it is trapped in a non-magnetic one, resulting in a lower vortex line energy and, thus, a stronger pinning potential.<sup>19</sup> Inset in Figure 1(c) displays the extra flux (generated by the stray field) that threads each Py dot, as a function of the external applied field. Even for low fields, this flux is not negligible and is comparable to  $\lambda$ , producing a substantial reduction of the supercurrents that explains the difference in pinning strengths between both samples. According to the figure, this difference is expected to increase with the applied field.

Fig. 3 shows the resistance as a function of the magnetic field for both samples. The Py dots sample shows much lower resistance for low applied fields due to the higher pinning strength. Surprisingly, as the magnetic field is increased, a crossover takes place with the Cu dots sample showing less resistance. This happens despite the fact that magnetic pinning is expected to increase its intensity with the magnetic field. Inset in Fig. 3 shows the critical temperature of both samples as a function of the magnetic fields; both samples display the

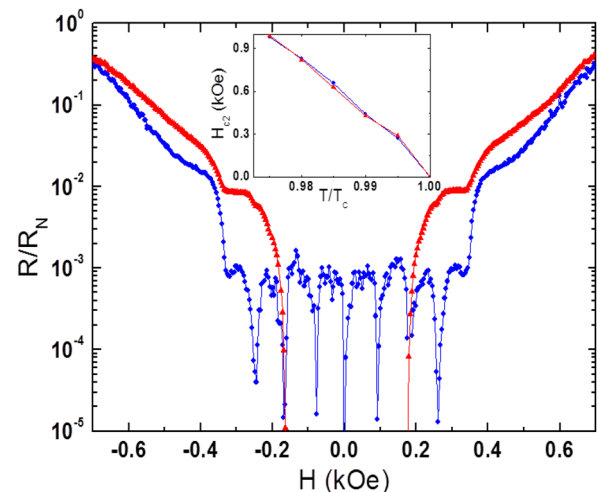


FIG. 3. Resistance as a function of the magnetic field for the Cu (blue dots) and Py (red triangles) nanodot samples, measured with 2.5 mA at  $0.975 T_c$ , with vortices pushed along the short side of the array. Inset:  $H_{c2}$  as a function of  $T/T_c$  for the Cu (blue dots) and Py (red triangles) nanodot samples. The high critical current for low fields in the Py dot sample has made the resistance too low to be measured.

same behavior. This situation rules out the possibility that increasing stray fields, generated by the Py dot, reduces the critical temperature of the film, leading to the observed crossover. The origin of this unexpected behavior must be on the vortex dynamics. The number  $n$  of vortices that can fit on a pinning site can be estimated by  $n = D/4\xi(T)$ , where  $D$  is the diameter of the dot and  $\xi(T)$  the coherence length.<sup>20</sup> In our case, in the temperature range in which electrical measurements can be properly performed (above  $0.9 T_C$ ), only one vortex fits on each dot, meaning that in the crossover region transport properties will be dominated by the interstitial vortices dynamics. As already pointed out, these vortices are not directly pinned and elastic strains avoid their motion when a Lorentz force is applied. These strains are a result of the repulsive force acting between the neighboring vortices

$$F_{1\rightarrow 2} = \frac{\phi_0}{4\pi} B_1(r) = \frac{\phi_0^2}{8\pi^2 \lambda_{eff}^2} K_0\left(\frac{r}{\lambda_{eff}}\right), \quad (1)$$

where  $B_1(r)$  is the magnetic field profile created by a vortex, and the zeroth-order Hankel function, which limits the range of the interaction to distances in the order of the effective penetration length,  $\lambda_{eff}$ .

As shown in the inset of Fig. 1(b), increasing the magnetic field swiftly increases the flux generated by stray fields. As a result, less supercurrents are needed to concentrate the magnetic field. In addition to this, the stray field outside the dot, which points in the opposite direction to the applied field, partially compensates its, further concentrating the magnetic field and effectively reducing the penetration length around the dot. This mechanism is depicted in the right inset of Fig. 4(a): i.e., the interaction between the stray field and the superconducting response leads to a more concentrated field profile. This vortex size shrinking has been predicted for magnetic superconductors with an intrinsic permeability<sup>21</sup> and has also been observed in the Ginzburg-Landau simulations of hybrid superconducting/magnetic systems similar to this one.<sup>22</sup> This vortex shrinking mechanism would be effective for both Abrikosov and Pearl vortices (in thinner films), although possibly to a different extent. The effective  $\lambda$  reduction yields important consequences in the vortex repulsive interaction, strengthening it for short distances but reducing its range. In general, the interaction becomes stronger for  $r < \lambda$  and weaker for  $r > \lambda$ .

Using the dirty limit approximation<sup>23</sup> and taking into account  $\xi_0 = 38$  nm for pure Nb,<sup>24</sup> data from the inset in Fig. 3 can be fitted to obtain the Ginzburg-Landau coherence length,  $\xi(0) = 9.8$  nm, and the mean free path,  $l = 3.5$  nm. Therefore, the penetration length of the Nb films can be estimated

$$\lambda(T) = 0.715 \frac{\lambda_L(0)}{l} \frac{\xi(0)}{\sqrt{1 - T/T_C}}, \quad (2)$$

where  $\lambda_L(0) = 23$  nm is the London penetration length.<sup>25</sup>

Fig. 4 shows the critical current in both samples as a function of the magnetic field when vortices are pushed along the two symmetry directions of the array, for a temperature  $T = 0.97 T_C$ , with  $\lambda = 275$  nm. As can be seen, the comparative field dependence is absolutely different

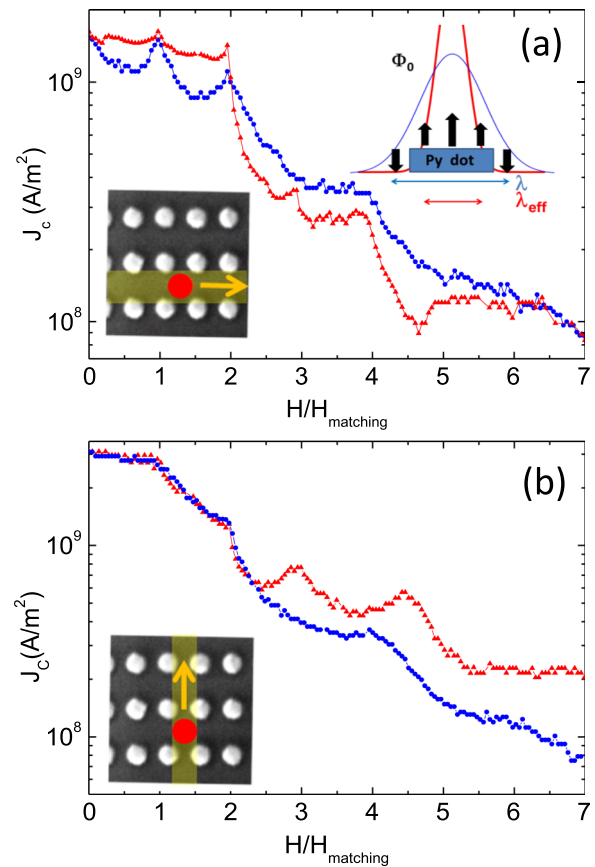


FIG. 4. Critical current as a function of the magnetic field for the Cu (blue dots) and Py (red triangles) nanodot samples, measured at  $0.975 T_C$ , with vortices pushed along the (a) short side of the array and (b) the long side of the array. Lower insets: Schematic description of the interstitial vortex (in red) motion (orange arrow) along the channels defined by the array (faded yellow). Upper inset panel: Schematic description of the  $\lambda$  reduction mechanism. The stray field (black arrows) interacts with the field profile created by the superconductor (blue), leading to a more concentrated resulting field distribution (red).

depending on the direction. It has been observed, both experimentally<sup>26</sup> and in simulations,<sup>27</sup> that after depinning, the interstitial vortices will start moving along the empty channels defined by the nanodot array in a plastic motion between rows of trapped vortices. The anisotropic shape of the nanodot array defines two channels, as depicted in the insets: a wide one within which the interstitials can flow far from the trapped vortices, keeping always a distance above  $\lambda$ ; and a narrow one, in which they are forced to move closer to them, at distances under  $\lambda$ . The effective  $\lambda$  reduction affects both situations very differently. In the first case, the repulsive interaction will become weaker, decreasing elastic strains along that direction. In that situation, the interstitial vortices can depin and start moving. This explains the crossover observed in the magnetoresistance measurements (see Fig. 4(a)). In the second case, repulsive interaction will become stronger, increasing elastic strains. This leads to the opposite situation, as showed in Fig. 4(b), and the critical current will increase with dot magnetization.

In summary, the use of magnetic nanostructures does not necessarily improve the transport properties of superconducting films. The stray fields created by these structures make them more efficient pinning centers than the non-

magnetic ones. However, magnetization can lead to an effective reduction of the penetration length, deeply affecting the dynamics of interstitial vortices. It has been found that this could enhance or depress transport properties at high fields, depending on the periodicity of the array,  $d$ . For separations  $d > \lambda$ , the vortex lattice becomes softer, interstitial vortices can move easier and the inclusion of magnetic nanostructures will negatively affect the electric performance. On the contrary, in more packed arrays,  $d < \lambda$ , magnetic character of the nanostructures considerably enhances the transport properties of the sample.

We thank the support from the Spanish Ministerio de Economía y Competitividad Grant No. FIS2013-45469 and CAM Grant No. P2013/MIT-2850 and EU COST Action MP1201.

- <sup>1</sup>M. Baert, V. V. Metlushko, R. Jonckheere, V. V. Moshchalkov, and Y. Bruynseraede, *Phys. Rev. Lett.* **74**, 3269 (1995); J. I. Martín, M. Vélez, A. Hoffmann, I. K. Schuller, and J. L. Vicent, *ibid.* **83**, 1022 (1999).
- <sup>2</sup>C. S. Lee, B. Jankó, I. Derényi, and A. L. Barabási, *Nature* **400**, 337 (1999); J. E. Villegas, S. Savel'ev, F. Nori, E. M. González, J. V. Anguita, R. García, and J. L. Vicent, *Science* **302**, 1188 (2003); Y. Togawa, K. Harada, T. Akashi, H. Kasai, T. Matsuda, F. Nori, A. Maeda, and A. Tonomura, *Phys. Rev. Lett.* **95**, 087002 (2005).
- <sup>3</sup>J. Trastoy, M. Malnou, C. Ulysse, R. Bernard, N. Bergeal, G. Faini, J. Lesueur, J. Briatico, and J. E. Villegas, *Nat. Nanotechnol.* **9**, 710 (2014).
- <sup>4</sup>J. E. Villegas, E. M. González, M. I. Montero, I. K. Schuller, and J. L. Vicent, *Phys. Rev. B* **68**, 224504 (2003); R. Wördenweber, P. Dymashevski, and V. R. Misko, *ibid.* **69**, 184504 (2004).
- <sup>5</sup>M. V. Milosevic, S. V. Yampolskii, and F. M. Peeters, *Phys. Rev. B* **66**, 174519 (2002); C. C. de Souza Silva, A. V. Silhanek, J. Van der Vondel, W. Gillijns, V. Metlushko, B. Ilic, and V. V. Moshchalkov, *Phys. Rev. Lett.* **98**, 117005 (2007); D. Perez de Lara, F. J. Castaño, B. G. Ng, H. S. Korner, R. K. Dumas, E. M. González, K. Liu, C. A. Ross, I. K. Schuller, and J. L. Vicent, *Appl. Phys. Lett.* **99**, 182509 (2011); A. Y. Aladyshkin, A. V. Silhanek, W. Gillijns, and V. V. Moshchalkov, *Supercond. Sci. Technol.* **22**, 053001 (2009).
- <sup>6</sup>M. Lange, M. J. Van Bael, Y. Bruynseraede, and V. V. Moshchalkov, *Phys. Rev. Lett.* **90**, 197006 (2003); M. V. Milosevic and F. M. Peeters, *Europhys. Lett.* **70**, 670 (2005); W. Gillijns, M. V. Milošević, A. V. Silhanek, V. V. Moshchalkov, and F. M. Peeters, *Phys. Rev. B* **76**, 184516 (2007); A. V. Silhanek, W. Gillijns, M. V. Milošević, A. Volodin, V. V. Moshchalkov, and F. M. Peeters, *ibid.* **76**, 100502(R) (2007).
- <sup>7</sup>J. S. Neal, M. V. Milošević, S. J. Bending, A. Potenza, L. San Emeterio, and C. H. Marrows, *Phys. Rev. Lett.* **99**, 127001 (2007); M. Iavarone, A. Scarfato, F. Bobba, M. Longobardi, G. Karapetrov, V. Novosad, V. Yefremenko, F. Giubileo, and A. M. Cucolo, *Phys. Rev. B* **84**, 024506 (2011).
- <sup>8</sup>M. V. Milošević and F. M. Peeters, *Phys. Rev. Lett.* **94**, 227001 (2005); V. N. Gladilin, J. Tempere, J. T. Devreese, W. Gillijns, and V. V. Moshchalkov, *Phys. Rev. B* **80**, 054503 (2009); D. A. Frotal, A. Chaves I, W. P. Ferreira I, G. A. Farias, and M. V. Milošević, *J. Appl. Phys.* **119**, 093912 (2016).
- <sup>9</sup>G. Karapetrov, J. Fedor, M. Iavarone, M. T. Marshall, and R. Divan, *Appl. Phys. Lett.* **87**, 162515 (2005); W. Gillijns, A. Y. Aladyshkin, M. Lange, M. J. Van Bael, and V. V. Moshchalkov, *Phys. Rev. Lett.* **95**, 227003 (2005).
- <sup>10</sup>N. Banerjee, C. B. Smiet, R. G. J. Smits, A. Ozaeta, F. S. Bergeret, M. G. Blamire, and J. W. A. Robinson, *Nat. Commun.* **5**, 3048 (2014); J. Linder and J. W. A. Robinson, *Nat. Phys.* **11**, 307 (2015); J. del Valle, A. Gómez, E. M. González, M. R. Osorio, D. Granados, and J. L. Vicent, *Sci. Rep.* **5**, 15210 (2015).
- <sup>11</sup>D. Ray, C. J. Olson Reichhardt, B. Jankó, and C. Reichhardt, *Phys. Rev. Lett.* **110**, 267001 (2013).
- <sup>12</sup>Y. L. Wang, M. L. Latimer, Z. L. Xiao, R. Divan, L. E. Ocola, G. W. Crabtree, and W. K. Kwok, *Phys. Rev. B* **87**, 220501 (2013); M. Motta, F. Colauto, W. A. Ortiz, J. Fritzsche, J. Cuppens, W. Gillijns, V. V. Moshchalkov, T. H. Johansen, A. Sánchez, and A. V. Silhanek, *Appl. Phys. Lett.* **102**, 212601 (2013); S. Guénon, Y. J. Rosen, A. C. Basaran, and I. K. Schuller, *ibid.* **102**, 252602 (2013).
- <sup>13</sup>D. J. Morgan and J. B. Ketterson, *Phys. Rev. Lett.* **80**, 3614 (1998).
- <sup>14</sup>A. Hoffmann, P. Prieto, and I. K. Schuller, *Phys. Rev. B* **61**, 6958 (2000).
- <sup>15</sup>M. Vélez, J. I. Martín, J. E. Villegas, A. Hoffmann, E. M. González, J. L. Vicent, and I. K. Schuller, *J. Magn. Magn. Mater.* **320**, 2547 (2008).
- <sup>16</sup>A. Gómez, D. Gilbert, E. M. González, K. Liu, and J. L. Vicent, *Appl. Phys. Lett.* **102**, 052601 (2013).
- <sup>17</sup>T. Shinjo, T. Okuno, R. Hassdorf, K. Shigeto, and T. Ono, *Science* **289**, 930 (2000).
- <sup>18</sup>J. E. Villegas, K. D. Smith, L. Huang, Y. Zhu, R. Morales, and I. K. Schuller, *Phys. Rev. B* **77**, 134510 (2008); M. V. Milosevic, F. M. Peeters, and B. Jankó, *Supercond. Sci. Technol.* **24**, 024001 (2011).
- <sup>19</sup>M. V. Milosevic and F. M. Peeters, *Phys. Rev. Lett.* **93**, 267006 (2004).
- <sup>20</sup>G. S. Mkrtchyan and V. V. Shmidt, *Sov. Phys. JETP* **34**, 195 (1972).
- <sup>21</sup>S. Z. Lin, L. N. Bulaevskii, and C. D. Batista, *Phys. Rev. B* **86**, 180506 (2012).
- <sup>22</sup>M. V. Milosevic and F. M. Peeters, *Phys. C* **404**, 246 (2004).
- <sup>23</sup>U. Welp, Z. L. Xiao, J. S. Jiang, V. K. Vlasko-Vlasov, S. D. Bader, G. W. Crabtree, J. Liang, H. Chik, and J. M. Xu, *Phys. Rev. B* **66**, 212507 (2002).
- <sup>24</sup>B. W. Maxfield and W. L. McLean, *Phys. Rev.* **139**, A1515 (1965).
- <sup>25</sup>A. Romanenko, A. Grassellino, F. Barkov, A. Suter, Z. Salman, and T. Prokscha, *Appl. Phys. Lett.* **104**, 072601 (2014).
- <sup>26</sup>K. Harada, O. Kamimura, H. Kasai, T. Matsuda, A. Tonomura, and V. V. Moshchalkov, *Science* **274**, 1167 (1996).
- <sup>27</sup>C. Reichhardt and C. J. Olson-Reichhardt, *Phys. Rev. B* **79**, 134501 (2009).